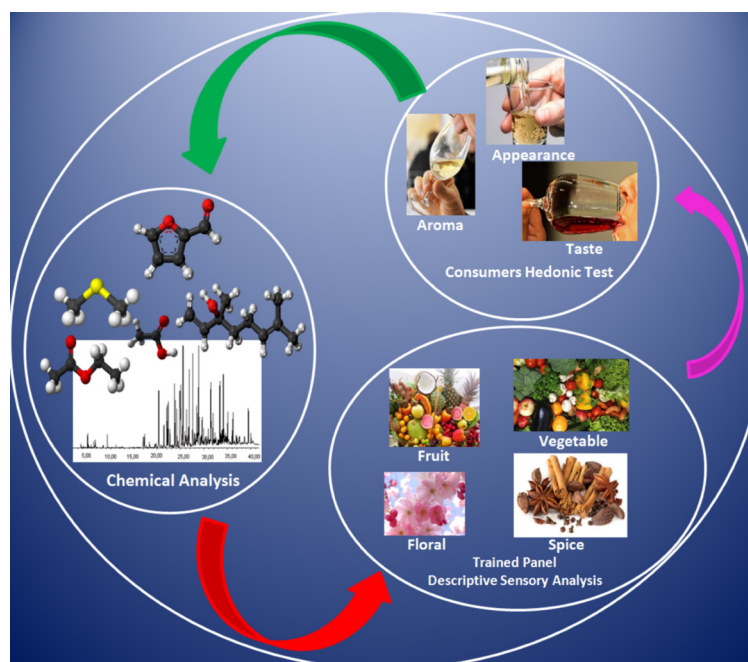


## Cover Picture



Chemical and sensory aspects of sugarcane spirits (*cachaças*) are described aiming to better understanding their sensory and chemical characteristics and their possible correlations. Chemometrics treatment of the beverage's chemical and sensory evaluation data provide a model to predict the *cachaça*'s quality and consumer's acceptance based on chemical descriptors. Details are presented in the Article **Correlation between Chemical Composition and Sensory Properties in Sugarcane Spirits** by Felipe A. T. Serafim, Fernanda R. F. Seixas, Alexandre A. Da Silva, Carlos A. Galinaro, Eduardo S. P. Nascimento, Silmara F. Buchviser, Luigi Odello and Douglas W. Franco on page 973.

## Contents

### Editorial

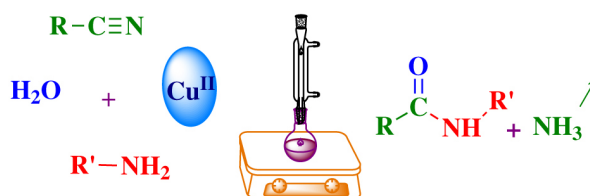
- 891 **From Submission to Publication: How We Work with Your Manuscript**  
Joaquim A. Nóbrega and Watson Loh

## Articles

### 895 Green and Selective Synthesis of *N*-Substituted Amides using Water Soluble Porphyrinato Copper(II) Catalyst

Sara S. E. Ghodsinia, Batool Akhlaghinia, Elham Safaei and Hossein Eshghi

SI online



R, R' = alkyl, aryl, heteroaryl

25 examples

#### Graphical Abstract

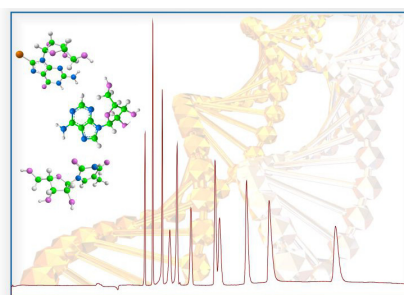
[Cu(2,3-tmtppa)](MeSO<sub>4</sub>)<sub>4</sub> efficiently catalyzes the direct conversion of nitriles to *N*-substituted amides with primary amines. The one pot selective synthesis of the *N*-substituted amide was performed in refluxing H<sub>2</sub>O

### 904 Development and Validation of a Micellar Electrokinetic Capillary Chromatographic Method for the Assessment of Nucleosides, Potential Biomarkers, in Blood Serum

Adriana Z. Buzatto, Sumaya F. Guedes, Lucas T. Vidotto, Laurione C. Oliveira and Ana Valéria C. Simionato

#### Graphical Abstract

The separation of ten modified nucleosides by capillary electrophoresis with UV detection (CE-UV) was accomplished by the use of an anionic surfactant in the background electrolyte, within 25 min and high efficiency (ca. 10<sup>5</sup>). The method presents appropriate detectability, linearity, precision and accuracy and may be applied for the analyses of blood samples from cancer patients



### 914 Ultrasound-Assisted Synthesis of 1-*N*-β-D-Glucopyranosyl-1*H*-1,2,3-triazole Benzoheterocycles and their Anti-Inflammatory Activities

Gilson B. da Silva, Bruna M. Guimarães, Shalom P. O. Assis, Vera L. M. Lima and Ronaldo N. de Oliveira

SI online



#### Graphical Abstract

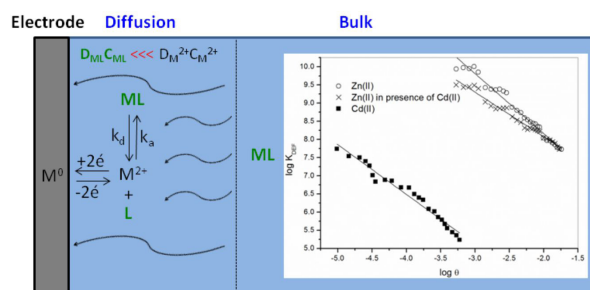
Glucopyranosyl-triazoles were synthesized in good yields under ultrasound activation. NOE experiments showed a solvent effect on the conformational equilibrium. The glucoheterocycles revealed potent anti-inflammatory activity

### 922 A Voltammetric Study on the Adsorption of Cd(II) and Zn(II) on Marine Microalgae *Tetraselmis gracilis* (Kyllin) Butcher

Kamila dos Santos Maguerroski, Marilda Rigobello-Masini and Jorge C. Masini

#### Graphical Abstract

Biosorption of Cd(II) and Zn(II) by the marine microalgae *T. gracilis* was studied. Adsorption capacity and binding stability were higher for Zn(II) in comparison with Cd(II). Zinc inhibited the adsorption of Cd(II), but minor adsorption sites with strong affinity for Cd(II) were observed, suggesting that under depletion of Zn(II), bioaccumulation of Cd(II) may occur

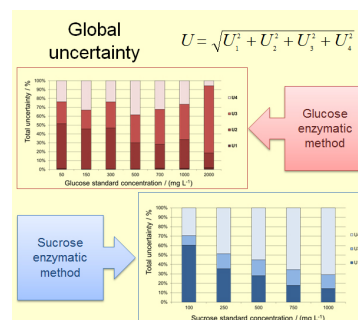


### 931 Uncertainty in the Determination of Glucose and Sucrose in Solutions with Chitosan by Enzymatic Methods

Berta N. Estevinho, Amélia Ferraz, Lúcia Santos, Fernando Rocha and Arminda Alves

#### Graphical Abstract

The global uncertainty (*U*) combines the contributions of all the sources of error linked to the analytical procedure. *U*<sub>1</sub>, *U*<sub>2</sub>, *U*<sub>3</sub> and *U*<sub>4</sub> are the uncertainties associated to standard preparation, calibration curve, precision and accuracy, respectively



**939 Investigation of the Interaction of Sertraline with Calf Thymus DNA by Spectroscopic Methods**

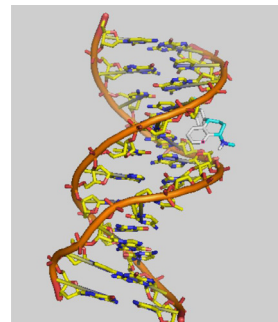


Parisa S. Dorraji and Fahimeh Jalali

SI online

**Graphical Abstract**

Sertraline, an antidepressant drug, has a high affinity with calf thymus DNA at physiological pH conditions. The interaction of sertraline with DNA was investigated by various methods. Minor-groove binding mode was concluded as a result of this study

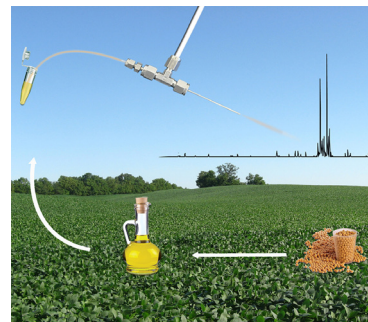


**946 Blends of Soybean Biodiesel with Petrodiesel: Direct Quantitation via Mass Spectrometry**

Patrícia V. Abdelnur, Sergio A. Saraiva, Rodrigo R. Catharino, Mirela Coelho, Nicolas Schwab, Camila M. Garcia, Ulf Schuchardt, Vanderléa de Souza and Marcos N. Eberlin

**Graphical Abstract**

Schematic representation of the Venturi easy ambient sonic-spray ionization in its liquid mode ( $V_L$ -EASI) analysis of Bn blends. A droplet of the Bn blend is diluted in acidified methanol and simply sprayed using a homemade  $V_L$ -EASI source for the direct mass spectrometric analysis



**953 Synthesis and Phytotoxic Activity of 1,2,3-Triazole Derivatives**



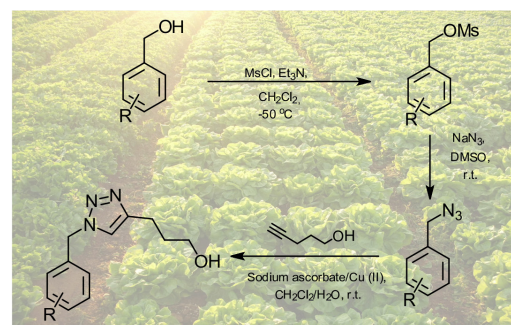
Thiago F. Borgati, Rosemeire B. Alves, Róbson R. Teixeira, Rossimiriam P. de Freitas, Thays G. Perdigão,

SI online

Silma F. da Silva, Aline Aparecida dos Santos and Alberto de Jesús O. Bastidas

**Graphical Abstract**

The increasing of herbicide resistant weeds has been stimulating researchers to find new chemical control agents. Within this context, heterocyclic compounds play an important role. Described in this work is the synthesis and phytotoxic evaluation of novel 1,2,3-triazole bearing halogenated benzyl moieties



**962 2D Chemometric Studies of a Series of Azole Derivatives Active against Fluconazole-Resistant *Cryptococcus gattii***

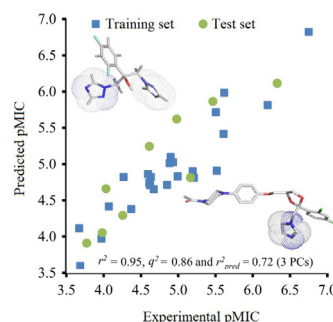


Humberto F. Freitas, Tania F. Barros and Marcelo S. Castilho

SI online

**Graphical Abstract**

Classification and quantitative models were developed to determine which features are relevant to the antifungal activity of a series of 33 azole derivatives assayed against *Cryptococcus gattii*. From these models, electronic characteristics were highlighted as important for antifungal activity and targeted to structural changes in this series of compounds



**973 Correlation between Chemical Composition and Sensory Properties of Brazilian Sugarcane Spirits (*Cachaças*)**



Felipe A. T. Serafim, Fernanda R. F. Seixas, Alexandre A. Da Silva, Carlos A. Galinaro, Eduardo S. P. Nascimento, Silmara F. Buchviser, Luigi Odello and Douglas W. Franco

SI online

**Graphical Abstract**

This manuscript describes the search for a correlation between 36 chemical compounds and 10 sensory attributes using principal components analysis. A chemical model was then developed using linear discriminant analysis and tested as an alternative tool to classify *cachaças* according to their sensory qualities

**Chemical and sensory analysis of sugarcane spirits**

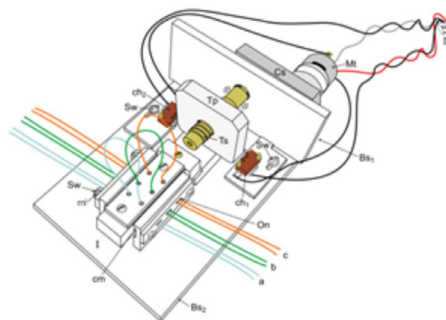


**983 Development of a New Version of an Automatic Commutator Injector and a Procedure for the Photometric Determination of Ethanol in Distilled Spirits**

Felisberto G. Santos and Boaventura F. Reis

**Graphical Abstract**

Figure presents an overview of the new version of the automatic injector showing its configuration ready to be used. This design facilitated the replacement of the movable part and contributed to reducing the friction, thereby allowing the use of a small DC motor to move the central piece from the sampling position to the injection position and vice versa

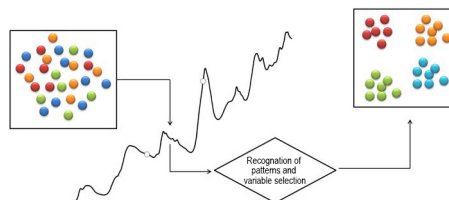


**991 Classification of Tablets containing Dipyron, Caffeine and Orphenadrine by Near Infrared Spectroscopy and Chemometric Tools**

Carlos Alan D. Melo, Priscila Silva, Adriano de Araújo Gomes, David Douglas S. Fernandes, Germano Vêras and Ana Claudia D. Medeiros

**Graphical Abstract**

A method is proposed for classifying drugs with dypirone, orphenadrine and caffeine. The chemometric models were SIMCA, GA-LDA and SPA-LDA with NIR spectroscopy. All models obtained 100% correct classification, using full, 12 and 2 variables. The results indicate potential for use as a tool in drug quality control

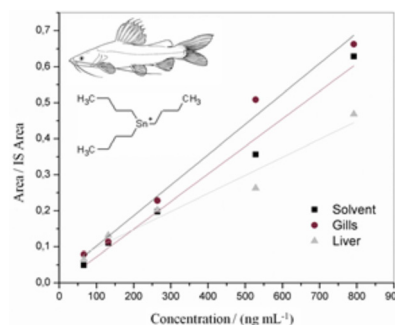


**998 Matrix Effect on Butyltin Analysis of Sediments and Fish Tissues by GC-PFPD**

Dayana M. dos Santos, Mary Rosa R. de Marchi, Ana Flávia L. Godoi, Alexander Turra and Rosalinda C. Montone

**Graphical Abstract**

Matrix effect can occur in chromatographic analysis of organotin compounds, such as tributyltin (TBT) by gas chromatography with pulsed flame photometric detection (GC-PFPD), mainly involving complex matrices, such as fish tissues, while it is not observed in abiotic samples



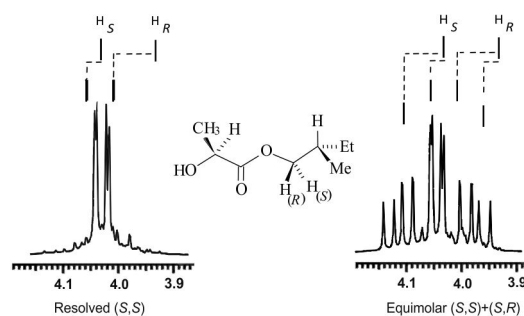
**1006 Absolute Configuration and Enantiomeric Composition of Partially Resolved Mandelic, Atrolactic and Lactic Acids by <sup>1</sup>H NMR of their (S)-2-Methylbutyl Esters**



SI online Francisco A. da C. Andrade, Maricleide P. de L. Mendes and Neuracy C. da Fonseca

**Graphical Abstract**

Configurations for the original acids were attributed, chemical shifts of the geminal protons were assigned and enantiomeric compositions were determined. The suggested structural model correlates the deshielding effects of the ethyl and methyl groups over the protons situated in the opposite face

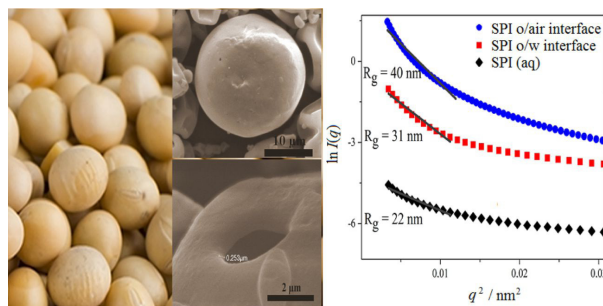


**1012 Morphology of Soy Protein Isolate at Oil/Water and Oil/Air Interfaces**

Samira J. Fayad, Betina G. Zanetti-Ramos, Pedro L. M. Barreto, Valdir Soldi and Edson Minatti

**Graphical Abstract**

Soy protein isolate (SPI) was used as an emulsifier for oil in water (o/w) emulsions to obtain microcapsules after drying. The results show that the morphology of the protein chains changed when nested at different interfaces and the capsule walls were made from the fractal aggregation of single chains

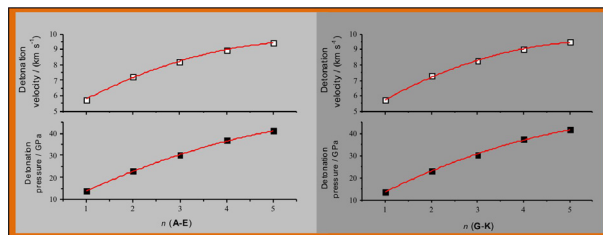




**1018 Theoretical Studies on High Energetic Density Polynitroimidazopyridines**  
Ming Lu and Guozheng Zhao

**Graphical Abstract**

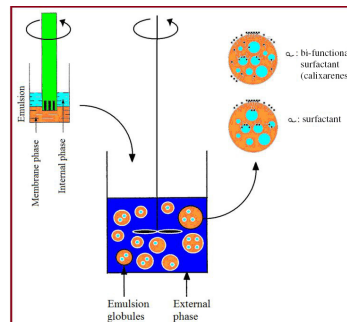
Density functional theory (DFT) was employed to study polynitroimidazopyridines at the B3LYP/6-31+G(d) level. The simulation results reveal that two molecules perform similarly to 1,3,5,7-tetranitro-1,3,5,7-tetrazocane (HMX), and other two molecules may be potential candidates for high energy density compounds (HEDCs)



**1027 Separation and Preconcentration of Dioxin in Blood Samples by Nano-baskets of Calixarene and Inclusion Emulsion Membranes**  
Bahram Mokhtari and Kobra Pourabdollah

**Graphical Abstract**

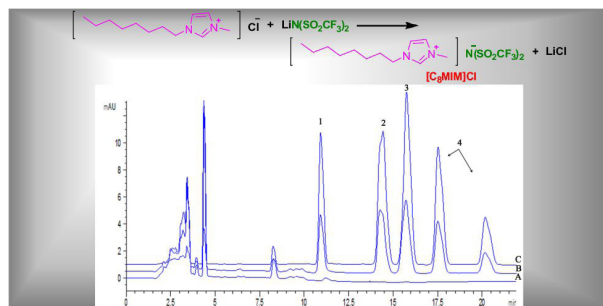
The novelty of this study is the application of nano-baskets of calixarene in the selective and efficient preconcentration and separation of dioxin. For this aim, four derivatives of *p*-tert-calix[4]arene bearing different sulfonamide moieties were synthesized and their inclusion-extraction parameters were optimized



**1034 An *in situ* Ionic Liquid Dispersive Liquid-Liquid Microextraction Method for the Detection of Pyrethroids by LC-UV in Environmental Water Samples**  
Chen Yu, Sanbing Zhang, Jiaheng Zhang, Songqing Li, Wenfeng Zhou, Haixiang Gao and Runhua Lu

**Graphical Abstract**

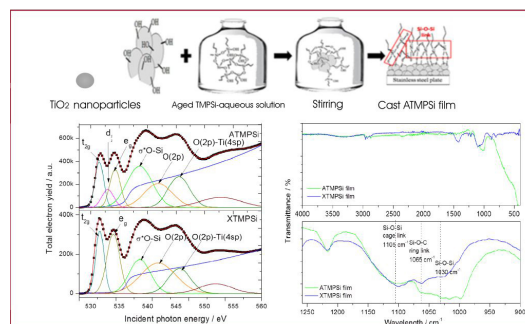
The remarkable advantage of *in situ* metathesis reaction assisted IL-DLLME is that it does not require the utilization of an organic disperser solvent. The typical chromatogram indicates that the matrix complexity had little effect on this method



**1041 NEXAFS and FTIR-ATR Investigation of the Static and Dynamic Superhydrophobicity of Functionalized Titanium Dioxide Nanoparticle Coatings**  
Rajajeyaganthan Ramanathan and Daniel E. Weibel

**Graphical Abstract**

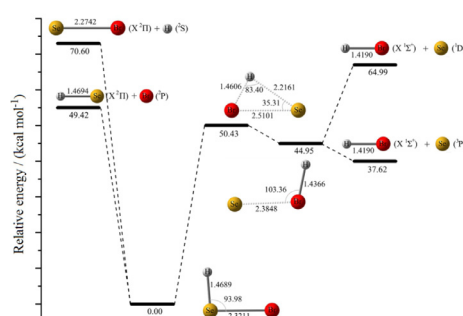
The superhydrophobic surfaces (static water contact angle (WCA)  $\geq 159^\circ$ ) fabricated using aqueous and non-aqueous solvents were probed in detail by NEXAFS and FTIR-ATR. The chemical heterogeneity of the surface determined the dynamic of the wetting phenomena without altering the static component of the superhydrophobicity



**1049 Characterizing New Molecular Species: A Systematic Study of Stationary States on the Singlet [H, Se, Br] Potential Energy Surface**  
William Hermoso, Debora B. Morf and Fernando R. Ornellas

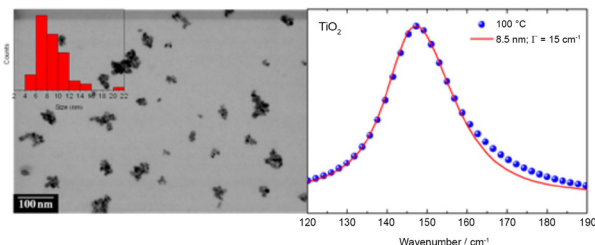
**Graphical Abstract**

Geometric parameters and energy profile showing the relative stability of the isomers HSeBr and HBrSe, the barrier height to isomerization and the dissociation channels



**1057 Phonon Confinement Model to Measure the Average Sizes of Anatase Nanoparticles Synthesized by a Solvothermal Method Using  $\text{H}_2\text{O}_2$**

SI online Bartolomeu C. Viana, Juliana Sousa Gonçalves, Valdemir dos Santos, Maria Rita de M. C. Santos, Elson Longo, Francisco E. P. Santos, and José Milton Elias de Matos



**Graphical Abstract**

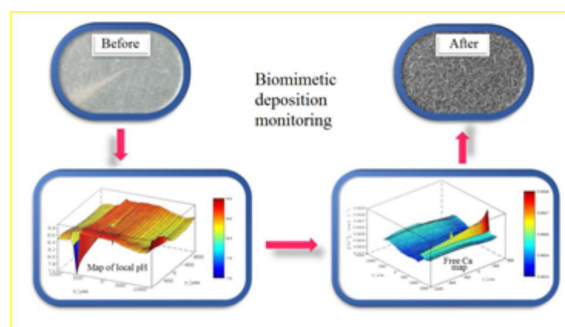
Anatase nanoparticle size measurements employed Raman spectroscopy and the phonon confinement model in comparison with TEM images and particle size distribution

**1064 Thermodynamic Simulation of Phosphate Precipitation based on Ion-Selective Microelectrode Measurements**

Gustavo M. Platt, Ivan N. Bastos, Mônica C. de Andrade, Marina Taryba, Sviatlana V. Lamaka, Alda Simões and Glória D. Soares

**Graphical Abstract**

Experimental monitoring and computational simulation of titanium surface modifications during biomimetic coating. Before: Bare titanium. The pH-microelectrode can be seen at 45° towards the center. After: Coated titanium



**1072 Determination of Nickel in Alcoholic Beverages by FAAS after online Preconcentration using Mandarin Peel (*Citrus reticulata*) as Biosorbent**

Gabriela C. Ribeiro, Luciana M. Coelho and Nívia M. Melo Coelho

**Graphical Abstract**

The figure shows mandarin orange (*Citrus reticulata*) used as a biosorbent in an on-line system coupled to flame atomic absorption spectrometry for the preconcentration and determination of nickel in alcoholic beverages

